Journal of Alloys and Compounds 527 (2012) 247–251

Contents lists available at SciVerse ScienceDirect

Journal of Alloys and Compounds

journal homepage: www.elsevier.com/locate/jallcom

Fabrication and thermal aging behavior of skutterudites with silica-based composite protective coatings

Hongliang Dong[a], Xiaoya Li[a], Yunshan Tang[a], Ji Zou[b], Xiangyang Huang[a], Yanfei Zhou[a], Wan Jiang[c], Guo-jun Zhang[b], Lidong Chen[a,*]

[a] CAS Key Laboratory of Materials for Energy Conversion, Shanghai Institute of Ceramics, Chinese Academy of Sciences, 1295 Dingxi Road, Shanghai 200050, China
[b] State Key Laboratory of High Performance Ceramics and Superfine Microstructure, Shanghai Institute of Ceramics, Chinese Academy of Sciences, 1295 Dingxi Road, Shanghai 200050, China
[c] College of Materials Science and Engineering, Donghua University, Shanghai 201620, China

ARTICLE INFO

Article history:
Received 20 December 2011
Received in revised form 15 February 2012
Accepted 17 February 2012
Available online xxx

Keywords:
Thermoelectric materials
Skutterudites
Silica-based composite coating
Slurry technology
Protective coating

ABSTRACT

Silica-based composite coatings with dispersion of glass or alumina granular particles were fabricated on n-type $Yb_{0.3}Co_4Sb_{12}$ and p-type $CeFe_3CoSb_{12}$ skutterudite (SKD) thermoelectric (TE) materials using hybrid silica sol as raw material which was synthesized through hydrolysis and condensation under acid condition process. The dispersion of either glass particles or alumina particles restrained the formation of micro-cracks during solidification due to relaxing tremendous cohesive stress in the gel. The high temperature stability for both the coating materials and the coated skutterudite matrix were investigated through thermal aging at 873 K in vacuum. Inter-diffusion of Sn from glass toward SKDs and Sb from SKDs toward coating layer was observed in the glass particle dispersed silica composite coating, which resulted in the failure of protecting function of the coating layer. In the alumina particle dispersed silica coating, neither diffusion nor reaction between the coating and SKD materials was observed after thermal aging at 873 K. The sublimation of antimony is suppressed in the SKDs overlaid by the alumina dispersed silica composite coating.

1. Introduction

Skutterudite-based (SKDs) thermoelectric (TE) materials and devices have been intensively studied in the past decades due to the potential of application for high temperature TE power generation [1–4]. The efficiency of TE materials is defined as $ZT = S^2\sigma T/\kappa$, where T, S, σ, and κ are the absolute temperature, Seebeck coefficient, electrical conductivity, and total thermal conductivity, respectively. Recently, great progresses have been achieved in the improvement of TE properties, and larger ZT_{max} up to 1.7 at 850 K was obtained in $Ba_uLa_vYb_wCo_4Sb_{12}$ triple-filled skutterudites [5]. However, there are still obstacles for realizing the practical application of SKD-based TE devices. For example, the skutterudite-based materials are inclined to volatilize or to be oxidized [6–14] at the service temperature, which will result in the degradation of TE performance. Wei et al. [7] investigated the stability of Ba and In double-filled SKDs by periodically quenching the samples from 723 K to room temperature, and found that the quenching treatment caused enrichment of Ba and loss of Sb and Co on the grain boundaries. Zhao et al. [8,9] studied the oxidation behavior of $CoSb_3$ in air from 773 K to 923 K and the sublimation behavior of antimony in $CoSb_3$ in vacuum from 873 K to 1023 K. They reported that the ZT_{max} decreased ~30% after oxidation at 923 K for 48 h or after thermal aging test of 16 days at 1023 K in vacuum. Hara et al. [10] reported that two layers of the oxidation products formed on the surface of the large size $CoSb_3$ samples in air at 873 K. Leszczynski et al. [11] observed that for $CoSb_3$, the oxidation starts at the temperature of 653 K, which was lower than that for CoP_3. Recently, Leszczynski et al. [12] studied the thermal durability of $CoSb_3$ in different atmospheres over the temperature range of 293–1123 K, and observed the formation of complex three-layer oxidation products of $CoSb_2O_4$, $CoSb_2O_6$ and Sb_2O_4 after oxidation in air. Sklad et al. [13] studied the stability of $CeFe_4Sb_{12}$ in air, and reported that the $CeFe_4Sb_{12}$ powder decomposed and then was rapidly oxidized above 573 K which is much lower than the device operating temperature at hot side. The results reported by Snyder and Caillat [14] show that $CoSb_3$ decomposes to $CoSb_2$, CoSb, and antimony vapor between 873 K and 973 K. Furthermore, the volatilized element can condense on the low temperature part which could result in the electrical and thermal short circuit. The thermal decomposition or sublimation and the oxidation are the major causes for the degradation of SKD materials at high temperature and the protection becomes the vital technique for developing SKD-based device.

* Corresponding author. Tel.: +86 21 52412550; fax: +86 21 52413122.
E-mail address: chenlidong@mail.sic.ac.cn (L. Chen).

0925-8388/$ – see front matter © 2012 Elsevier B.V. All rights reserved.
doi:10.1016/j.jallcom.2012.02.116

The most effective and convenient approach to prevent the TE performance degradation of SKD materials at high temperature caused by Sb sublimation and/or oxidation is sealing the materials or the device into a closed environment such as fabricating a dense protective coating directly on the surface of SKD materials. Cr–5Si thin layers [15] onto $CoSb_3$ deposited by pulse magnetron sputtering was used to deter the degradation of skutterudite at elevated temperatures in air, but the thin layers lost protection function at 873 K. El-Genk and Saber et al. [16–18] reported the effectiveness of metallic (Mo, V, Ta, Ti) coatings on suppressing the sublimation of Sb from $CoSb_3$-based skutterudites. Sakamoto et al. [19] used a continuous metal foil as a physical barrier to suppress thermal decomposition near the surface of SKD thermoelectric materials. However, most metals would be reactive to antimony at high temperature and the current leakage through the metal film could decrease the device efficiency. Generally speaking, most of the metallic coatings by sputtering are poorly adhesive to SKDs, otherwise significant inter-diffusion and reaction between the coating and the substrate would not be avoided [20]. Recently, a thick aerogel coating [21] is developed to prevent the sublimation of Sb in vacuum. However, the brittleness of aerogel may result in the formation of microcracks, and the low compactness would decrease the effect on suppressing the sublimation of antimony in SKDs as silica aerogel is porous, weak and tenuous. Although lots of efforts have been focused on the protection of SKDs, the problem of sublimation and oxidation of SKDs has still not been solved thoroughly. The aim of the present work is to develop a novel silica-based composite protective coating for skutterudite thermoelectric materials. A modified sol–gel procedure combined with a slurry-blade method was used as a coating technique. The physical and chemical compatibility of coating-to-matrix was investigated systematically.

2. Experimental procedure

Bulk skutterudite materials with the nominal composition $CeFe_3CoSb_{12}$ and $Yb_{0.3}Co_4Sb_{12}$ were synthesized by melting, quenching, annealing and spark plasma sintering (SPS) processes. Commercial silica sol (30 wt% silica) and methyltriethoxysilane ($SiCH_3(OC_2H_5)$, MTES) were mixed evenly and then transparent sol was obtained through hydrolysis and polycondensation process at about pH = 2 adjusted by 1 M HCl solution. Coating slurry was obtained by mixing uniformly hybrid sol, glass frit (main chemical components: SnO and P_2O_5 small amount of ZnO and SiO_2) or alumina particles and solvent (ethyl alcohol, ETOH) in weight ratio of (60–70%):(30–40%):(1–10%). As for the Al_2O_3 dispersed system, silica aerogel was added into the slurry with an additive amount of 1 wt% of the amount of Al_2O_3. The hand-polished SKDs (square cube: 4 mm × 4 mm × 4 mm) specimens were coated through a slurry-blade method. The silica-based composite coatings were obtained by subsequent solidification at 373 K for 10 h in vacuum.

The thermal behavior of the hybrid silica material in air was simultaneously monitored with TG–DTA (STA429C, Netzsch) after preheating treatment at 373 K. The specimen was heated to 1273 K at a constant heating rate of 10 K min^{-1} in air. A Nicolet Fourier Transformation Infrared spectrophotometer was used to run Fourier transform infrared (FT-IR) experiments. Hybrid silica coating materials without glass powder dried at 373 K in air were ground with KBr and pressed into pellets for FT-IR measurement. Surface morphologies of the hybrid coatings were observed by SEM (JEOL JSM-6390) and the interface composition between the hybrid silica-based coating and skutterudite matrix was analyzed by electron probe X-ray micro-analyzer (EPMA) using JEOL JXA 8100 equipped with INCA-OXFORD energy dispersive spectroscopy (EDS).

3. Results and discussion

Fig. 1 shows the comparison of the Fourier transform infrared (FT-IR) spectra of hybrid silica powder and the silica powder obtained directly by drying hybrid silica sol and commercial silica sol, respectively. The hybrid silica sol was fabricated by hydrolysis and condensation process of MTES and silica sol. The broaden stretching vibration peak of O—H in the range from 3100 cm^{-1} to 3700 cm^{-1} [22] and the characteristic peak of the flexural vibration of hydroxyl in H_2O at about 1630 cm^{-1} due to the adsorbed water or

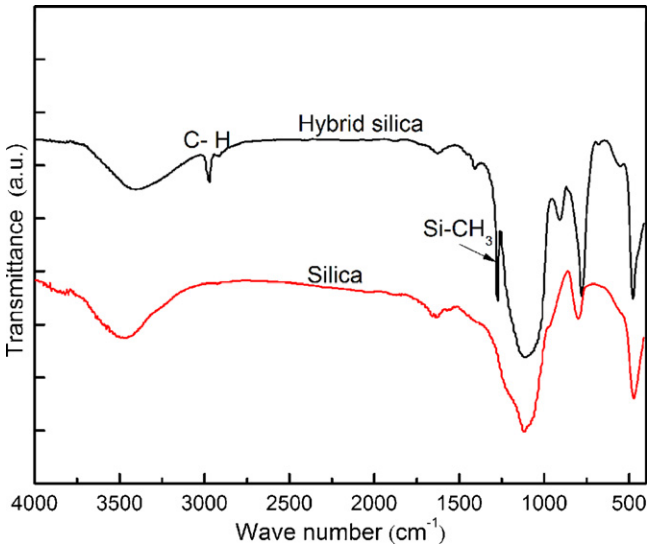

Fig. 1. Comparison of FT-IR spectra between hybrid silica material and silica from silica sol.

constituent water are observed in both of the silica and hybrid silica. The broad peak between 1000 cm^{-1} and 1250 cm^{-1} corresponds to Si—O absorption. The weak absorption peak of Si—OH at 906 cm^{-1} existing in the silica spectrum can hardly be identified in the hybrid silica spectrum due to involving in Si—O—Si absorption band. As compared with pure silica powder, some extra absorption peaks were observed in the hybrid silica. They occur at approximately 2970 cm^{-1}, 1400 cm^{-1}, 1273 cm^{-1} and 779 cm^{-1}, corresponding to the C—H stretching vibration mode, CH_3 and CH_2 bending mode, the Si—CH_3 strong and sharp absorption peak and a weak absorption peak [23], respectively. The existence of these absorption peaks indicates that Si—O—Si network was successfully modified by —CH_3 forming a hybrid network.

Fig. 2 shows the TG–DTA curves of the hybrid silica powder. The TG curve reveals the existence of three mass loss steps. The first one was caused by the evaporation of absorbed water at about 370 K with less than 2% mass loss. The second process is in the range of 423–573 K with about 8% mass loss. The third one begins at approximately 800 K with further ~7% mass loss. Two exothermal peaks are observed at about 563 K and 812 K, respectively. These two exothermic peaks correspond to the two large weight loss processes as shown by TG curve. Combining the TG and DTA analyses, we can conclude that the mass loss at ~563 K is due to the

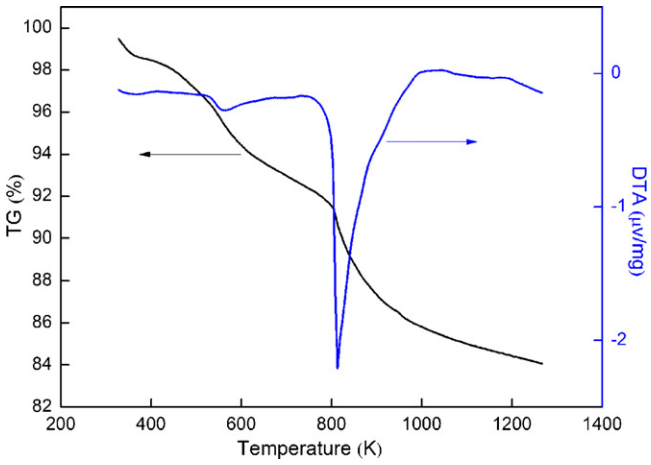

Fig. 2. TG–DTA plots of hybrid silica coating material.

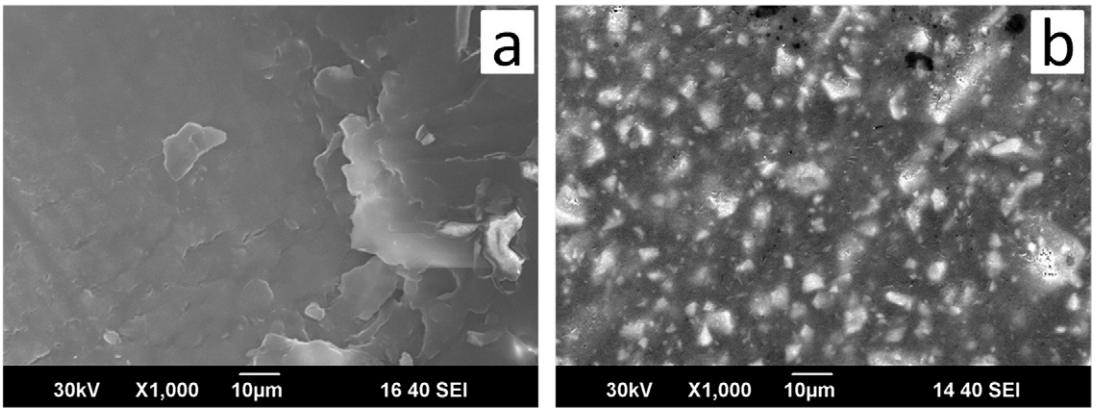

Fig. 3. Surface microstructure of hybrid coatings without (a) and with (b) glass powder.

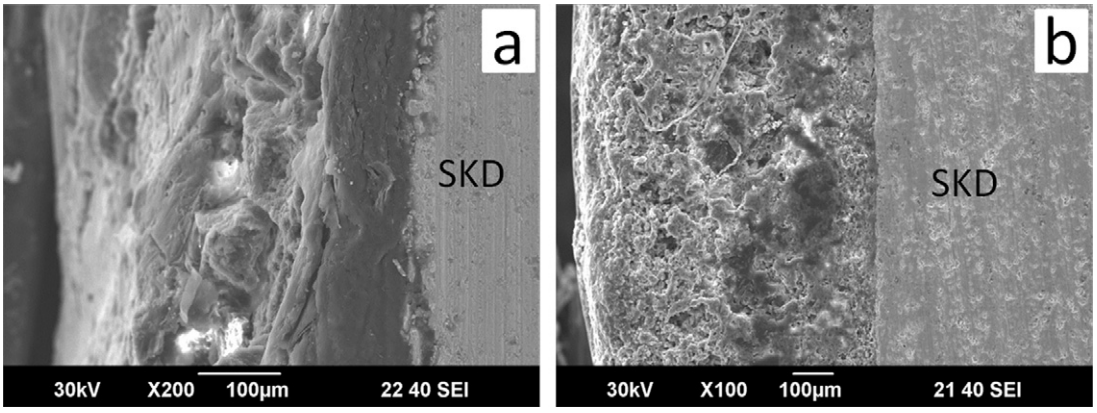

Fig. 4. Cross sectional morphologies of $CeFe_3CoSb_{12}$ coated by (a) hybrid silica and (b) glass frit-hybrid silica composite system.

combustion of residual Si—OH and the third weight loss at ~812 K is typically attributed to the combustion of residual organic radicals such as $-CH_3$.

Fig. 3 displays the natural surface morphologies of the hybrid silica and glass-hybrid silica composite coatings, and Fig. 4 shows the cross sectional morphologies of the coated $CeFe_3CoSb_{12}$ specimens. As observed by SEM, both the glass-hybrid silica and hybrid silica coatings are dense (Fig. 3(a) and (b)). This demonstrates the effectiveness of $-CH_3$ contained in the Si—O—Si hybrid network on relaxing the cohesive stress in the gel during solidification. The particle size of the glass powder in the coatings distributes in a wide range and the shape of particles is close to angular (Fig. 3(b)). Broadly speaking, thick films are difficult to be obtained via sol–gel method [24,25]. However, hybrid silica sol modified by organics has a clear advantage in preparing thick, crack free coatings [26]. At the same time, the slurry-blade method offers relatively thick hybrid silica coatings in comparison to dip or spin coating methods. The thick hybrid silica coatings can be effective for protecting the antimony sublimation from SKDs. However, peeling-off occasionally occurred in cutting process for hybrid silica coating without fillings, while thicker coating layers without cracks or peeling off were obtained for glass frit-hybrid silica coating system. The coating thickness can reach ~600 μm for glass frit-hybrid silica coating system.

Fig. 5(a) exhibits that the coating is still dense and crack-free after heat treatment at 873 K for 2 h in vacuum. Good adhesion between the glass-hybrid silica coating and the SKD matrix was realized. In fact, the softening phosphate glass is a good inorganic binder at high temperature. In the glass-hybrid silica coating, no cracks were found even after the heat treatment

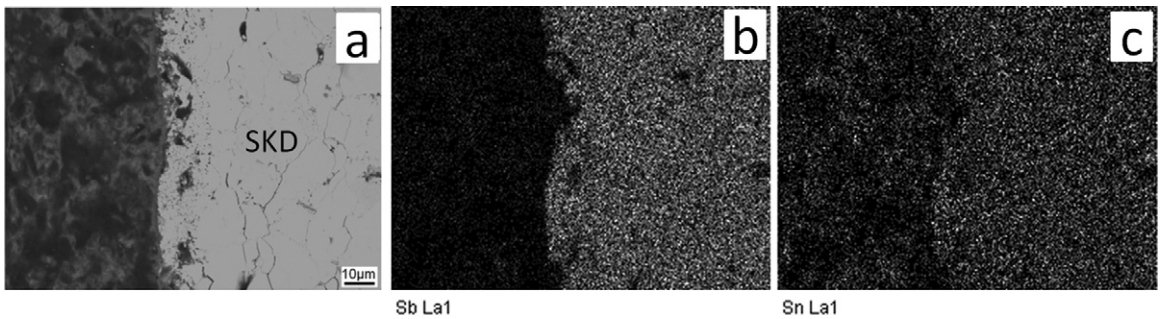

Fig. 5. Polished cross sectional morphology (a) and EDS spectra (b, Sb mapping spectrum of (a) and c, Sn mapping spectrum of (a)) of the interface between the glass-hybrid silica overlay coating and $CeFe_3CoSb_{12}$ matrix after heat treatment at 873 K for 2 h in vacuum.

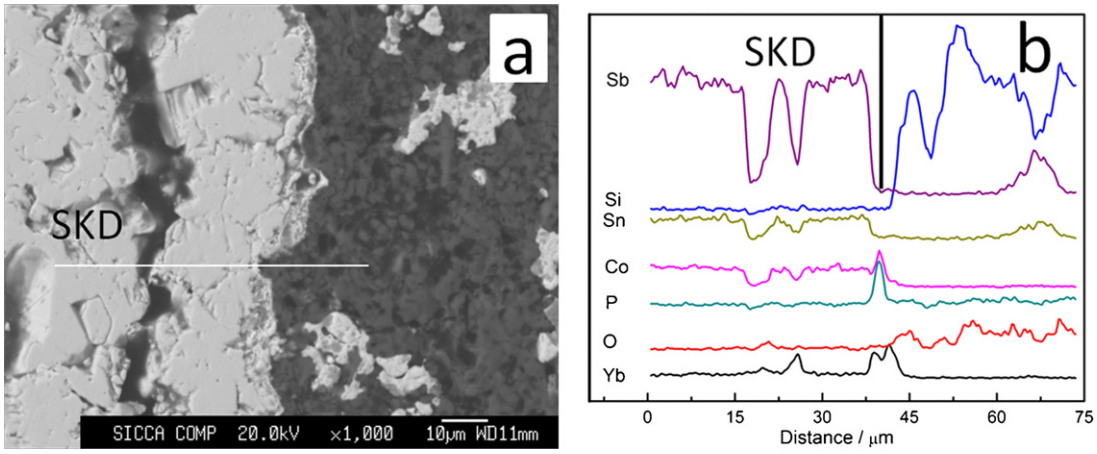

Fig. 6. SEM image (a) and EPMA line scan spectra (b) across the interface of the glass-silica coating and $CeFe_3CoSb_{12}$ matrix after heat treatment at 873 K for 62 h in vacuum.

at 873 K because the distribution of glass would tune the coefficient of thermal expansion (CTE) of coating to match the SKDs (CTE: glass $9–10 \times 10^{-6}\,K^{-1}$, silica $0.5 \times 10^{-6}\,K^{-1}$, $Yb_{0.3}Co_4Sb_{12}$ $10–11 \times 10^{-6}\,K^{-1}$, $CeFe_3CoSb_{12}$ $10–13 \times 10^{-6}\,K^{-1}$) which would decrease the thermal stress. Similar results as obtained in glass frit containing composite coating were also obtained in alumina-hybrid silica composite coating. From the view of tuning CTE and slurry viscosity, the dispersion of glass frit or alumina particles is benefited to fabricate thicker hybrid silica coating without formation of micro-cracks. However, Fig. 5(c) indicates that plenty of tin atoms have diffused into SKD matrix from glass-hybrid silica composite coating, while the outward diffusion of antimony into the coating is not so obvious (Fig. 5(b)). As SnO is the network modifier in the glass, when the temperature was enhanced to 873 K, the network would be relaxed, and the interaction between Sn- and network become weak which makes the Sn diffusion into SKD matrix more easily. In principle, Sn can substitute Sb in antimonide SKDs, and generate excess charge carrier (holes) in skutterudites

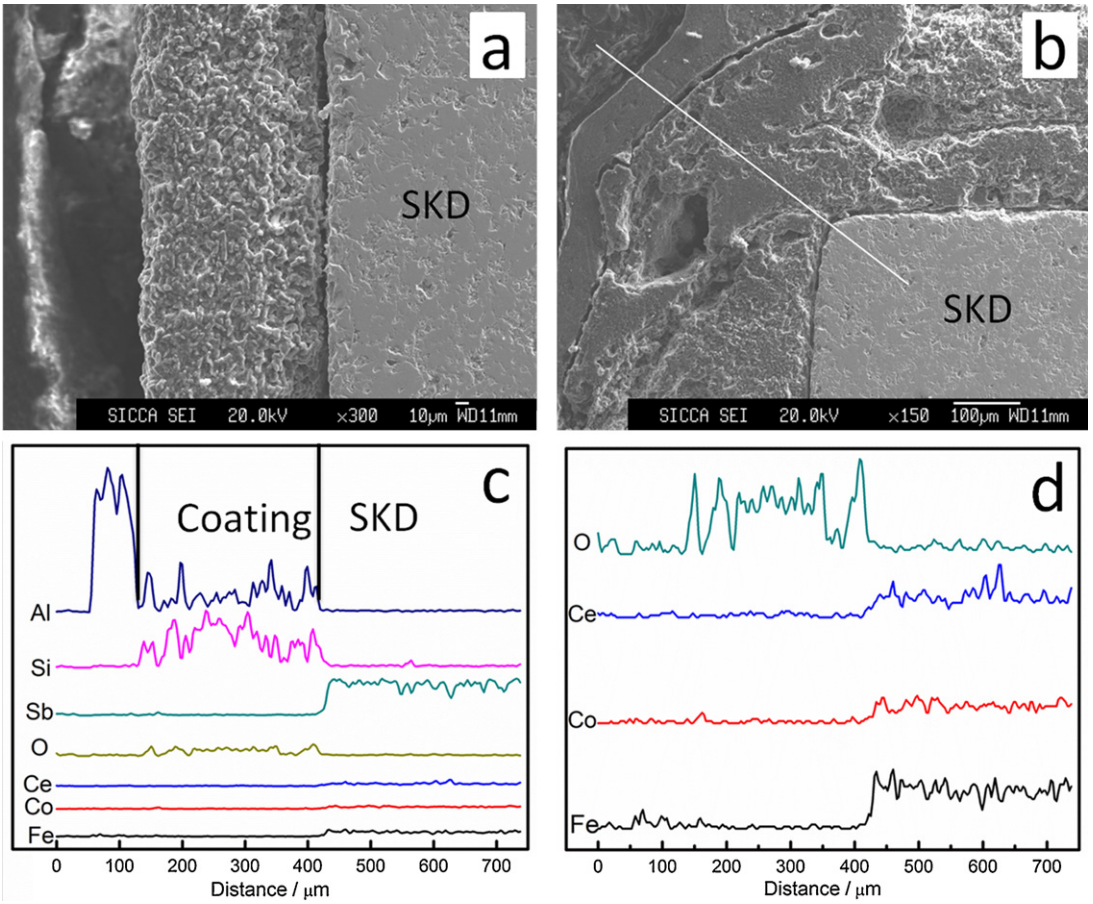

Fig. 7. Cross sectional images (a, b) and EPMA line scan (c, d). (d) shows higher magnification image of O, Ca, Co, Fe in (c) along the white line indicated in (b) for alumina-hybrid silica coated $CeFe_3CoSb_{12}$ after heat treatment at 873 K for 62 h in vacuum.

[27,28]. Therefore the diffusion of Sn into SKDs will greatly affect the TE properties of skutterudites. When the duration time at 873 K was extended to 62 h, the formation of Sn—Sb alloy was found in the glass-hybrid silica coating (Fig. 6). It can be easily explained because Sn and Sb are prone to react forming Sn—Sb compound or alloy according to the Sn—Sb phase diagram [29]. The EDS line scan presented in Fig. 6(b) obviously displays the variation of Sb and Sn in the range over the SKDs and the glass-silica composite coating system. In addition, there is a small amount of Co—P reaction product observed between the interface due to the depolymerization of PO_4 tetrahedron building unit in glass frit [30–32] and the outward diffusion of Sb from the surface of $Yb_{0.3}Co_4Sb_{12}$ SKD. According to the above observation, it can be concluded that the glass frit-contained hybrid silica coating would lose its protection function at high temperatures.

The thermal aging behavior of the p-type and n-type SKDs deposited by alumina contained hybrid silica coating was also examined. Fig. 7 presents the cross sectional microstructure and EPMA line scan profile across the interface between the alumina-silica composite coating and $CeFe_3CoSb_{12}$ matrix. In order to eliminate the influence of the fabrication process of the polished samples, the specimens were wrapped inside an aluminum foil. This resulted in the Al peak in the left side of EPMA line scan spectra. In contrast to the glass-silica composite coating, the components in the Al_2O_3–silica composite coating are particularly stable. EPMA line scan profile (Fig. 7(c)) shows that there is no diffusion between the alumina-hybrid silica coating and SKDs matrix. The adhesion between the $CeFe_3CoSb_{12}$ and the composite coating is robust even there is a hair-line crack occurring at the interface after long term thermal aging test. The Al_2O_3-hybrid silica composite coating is effective to block Sb from $CoSb_3$-based SKDs.

4. Conclusions

Inorganic–organic hybrid silica was successfully fabricated via a hydrolysis and condensation process using MTES and commercial silica sol as raw materials. The hybrid silica coatings with and without glass frit/alumina particles have been fabricated on SKDs (e.g. $CeFe_3CoSb_{12}$, $Yb_{0.3}Co_4Sb_{12}$) TE materials. With the distribution of glass frit or alumina particles in the hybrid silica sol, thick and dense coatings were obtained without the formation of micro-cracks. The diffusion of Sn and P into the skutterudite matrix forming interlayer can enhance the adhesion between the coating and SKD substrate. However, for the glass frit-hybrid silica composite coating, as increasing the thermal aging time, the interdiffusion of Sb and Sn would cause the composition variation and degradation of SKDs TE performance and thus result in the failure of protective function. The composite coating comprised of Al_2O_3 and modified silica is stable enough to resist the corrosion of Sb, and to block the sublimation of antimony from skutterudites.

Acknowledgments

The authors acknowledge financial support from the National High Technology Research and Development Program of China (No. 2009AA03Z210), National Natural Science Foundation of China (Project No. 50972158), Program of Shanghai Subject Chief Scientist (09XD1404400) and the Shanghai Committee of Science and Technology, China (Grant No. 10JC1400500).

References

[1] B.C. Sales, D. Mandrus, R.K. Williams, Science 272 (1996) 1325–1328.
[2] G.S. Nolas, M. Kaeser, R.T. Littleton, T.M. Tritt, Appl. Phys. Lett. 77 (2000) 1855–1857.
[3] L.D. Chen, T. Kawahara, X.F. Tang, T. Goto, T. Hiral, J.S. Dyck, W. Chen, C. Uher, J. Appl. Phys. 90 (2001) 1864–1868.
[4] H. Li, X.F. Tang, Q.J. Zhang, C. Uher, Appl. Phys. Lett. 93 (2008), 252109-1–252109-3.
[5] X. Shi, J. Yang, J.R. Salvador, M.F. Chi, J.Y. Cho, H. Wang, S.Q. Bai, J.H. Yang, W.Q. Zhang, L.D. Chen, J. Am. Chem. Soc. 133 (2011) 7837–7846.
[6] E. Godlewska, K. Zawadzka, A. Adamczyk, M. Mitoraj, K. Mars, Oxid. Met. 74 (2010) 113–124.
[7] P. Wei, W.Y. Zhao, C.L. Dong, X. Yang, J. Yu, Q.J. Zhang, Acta Mater. 59 (2011) 3244–3254.
[8] D. Zhao, C. Tian, S. Tang, Y. Liu, L. Chen, J. Alloy. Compd. 504 (2010) 552–558.
[9] D. Zhao, C. Tian, Y. Liu, C. Zhan, L. Chen, J. Alloy. Compd. 509 (2011) 3166–3171.
[10] R. Hara, S. Inoue, H.T. Kaibe, S. Sano, J. Alloy. Compd. 349 (2003) 297–301.
[11] J. Leszczynski, A.L. Malecki, T.K. Wojciechowski, Proceedings of the 5th European Conference on Thermoelectrics, Odessa, Ukraine, September 10–12, 2007, 2007.
[12] J. Leszczynski, T.K. Wojciechowski, A.L. Malecki, J. Therm. Anal. Calorim. 105 (2011) 211–222.
[13] A.C. Sklad, M.W. Gaultois, A.P. Grosvenor, J. Alloy. Compd. 505 (2010) L6–L9.
[14] G.J. Snyder, T. Caillat, High Efficiency Thermoelectrics Workshop San Diego, California February 17–20, 2004, http://www.thermoelectrics.caltech.edu/thermoelectrics/engineering.html.
[15] E. Godlewska, K. Zawadzka, K. Mars, R. Mania, K. Wojciechowski, A. Opoka, Oxid. Met. 74 (2010) 205–213.
[16] M.S. El-Genk, H.H. Saber, T. Caillat, J. Sakamoto, Energy Convers. Manage. 47 (2006) 174–200.
[17] H.H. Saber, M.S. El-Genk, T. Caillat, Energy Convers. Manage. 48 (2007) 555–567.
[18] H.H. Saber, M.S. El-Genk, Energy Convers. Manage. 48 (2007) 1383–1400.
[19] J.S. Sakamoto, T. Caillat, J.P. Fleurial, G.J. Snyder. United States Patent, No.: US 7,480,984 B1, Date of Patent: Jan. 27, 2009.
[20] M.S. Chu, S.K. Wu, Surf. Coat. Technol. 179 (2004) 257–264.
[21] J.S. Sakamoto, G.J. Snyder, T. Calliat, J.-P. Fleurial, S.M. Jones, J.-A. Palk. United States Patent, No.: US 7,461,512 B2, 9 Dec 2008.
[22] S. Yu, T.K.S. Wong, X. Hu, T.K. Goh, Thin Solid Films 306 (2004) 462–463.
[23] Z. Zhang, Y. Tanigami, R. Terai, H. Wakabayashi, J. Non-Cryst. Solids 189 (1995) 212–217.
[24] M. Takemori, Ceram. Int. 35 (2009) 1731–1746.
[25] A.K. Burrell, T.M. McCleskey, Q.X. Jia, Chem. Commun. (2008) 1271–1277.
[26] S. Ono, H. Tsuge, Y. Nishi, S. Hirano, J. Sol-Gel Sci. Technol. 29 (2004) 147–153.
[27] K.H. Park, S.C. Ur, I.H. Kim, J. Korean Phys. Soc. 57 (2010) 1000–1004.
[28] P. Qiu, X. Shi, X. Chen, X. Huang, R. Liu, L. Chen, J. Alloy. Compd. 509 (2011) 1101–1105.
[29] S.W. Chen, C.C. Chen, W. Gierlotka, A.R. Zi, P.Y. Chen, H.J. Wu, J. Electron. Mater. 37 (2008) 992–1002.
[30] A.E.R. Westman, P.A. Gartaganis, J. Am. Ceram. Soc. 40 (1957) 293–299.
[31] T.R. Meadowcroft, F.D. Richardson, Trans. Faraday Soc. 61 (1965) 54–70.
[32] R.K. Brow, J. Non-Cryst. Solids 263&264 (2000) 1–28.